

Supplementary information

Porous calcium-manganese oxide/carbon nanotube microspheres as efficient oxygen reduction catalysts for rechargeable zinc air batteries

Nguk Neng Tham¹, Xiaoming Ge¹, Aishui Yu², Bing Li^{1,3}, Yun Zong^{1*}, Zhaolin Liu^{1*}

¹Institute of Materials Research and Engineering (IMRE), A*STAR (Agency for Science, Technology and Research), 2 Fusionopolis Way, Innovis, #08-03, Singapore 138634, Republic of Singapore. Email: zl-liu@imre.a-star.edu.sg

²Department of Chemistry, Shanghai Key Laboratory of Molecular Catalysis and Innovative Materials, Institute of New Energy, Fudan University, Shanghai 200438, China

³School of Chemistry and Chemical Engineering, Harbin Institute of Technology, Harbin 150001, China

Contents

1. Fig. S1 SEM image of the carbonate precursor, $\text{CaMn}(\text{CO}_3)_2$	S2
2. Fig. S2 XRD pattern of $\text{CaMn}(\text{CO}_3)_2$ and its standard, PDF #84-1290	S3
3. Fig. S3 TEM and HRTEM images of CaMnO_3	S4
4. Fig. S4 TGA profile of CaMnO_3 , CMO/CNT and carbon nanotubes in air	S5
5. Fig. S5 Nyquist plot of zinc-air batteries with CMO/CNT-4, CMO/CNT-0.25 and Pt/C	S6
6. Fig. S6 Cycling stability performance of CMO/CNT-0.25 during galvanostatic recurrent pulse cycling test	S7
7. Table S1 Tabulated data for oxygen reduction reaction of the various electrocatalysts, with Pt/C as the benchmark	S8

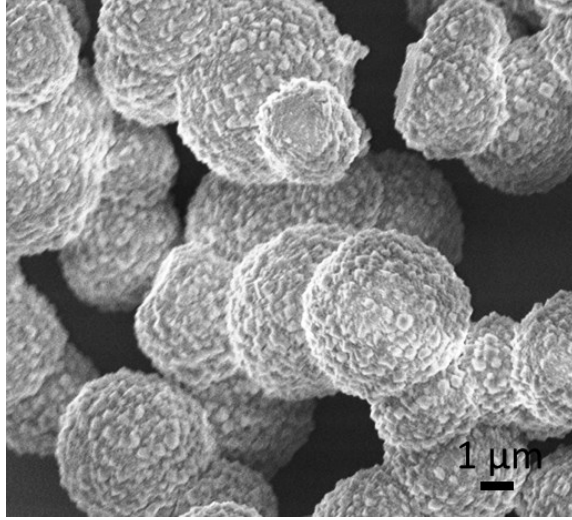


Fig. S1 SEM image of the carbonate precursor, CaMn(CO₃)₂.

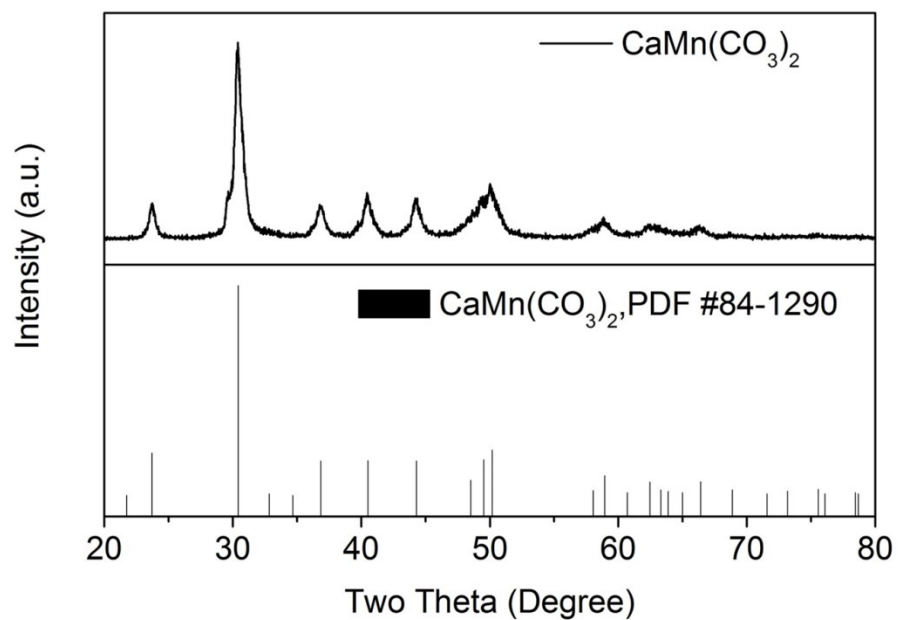


Fig. S2 XRD pattern of $\text{CaMn}(\text{CO}_3)_2$ and its standard, PDF #84-1290

The presence of $\text{CaMn}(\text{CO}_3)_2$ is further confirmed by XRD which corresponds to the standard (PDF #84-1290).

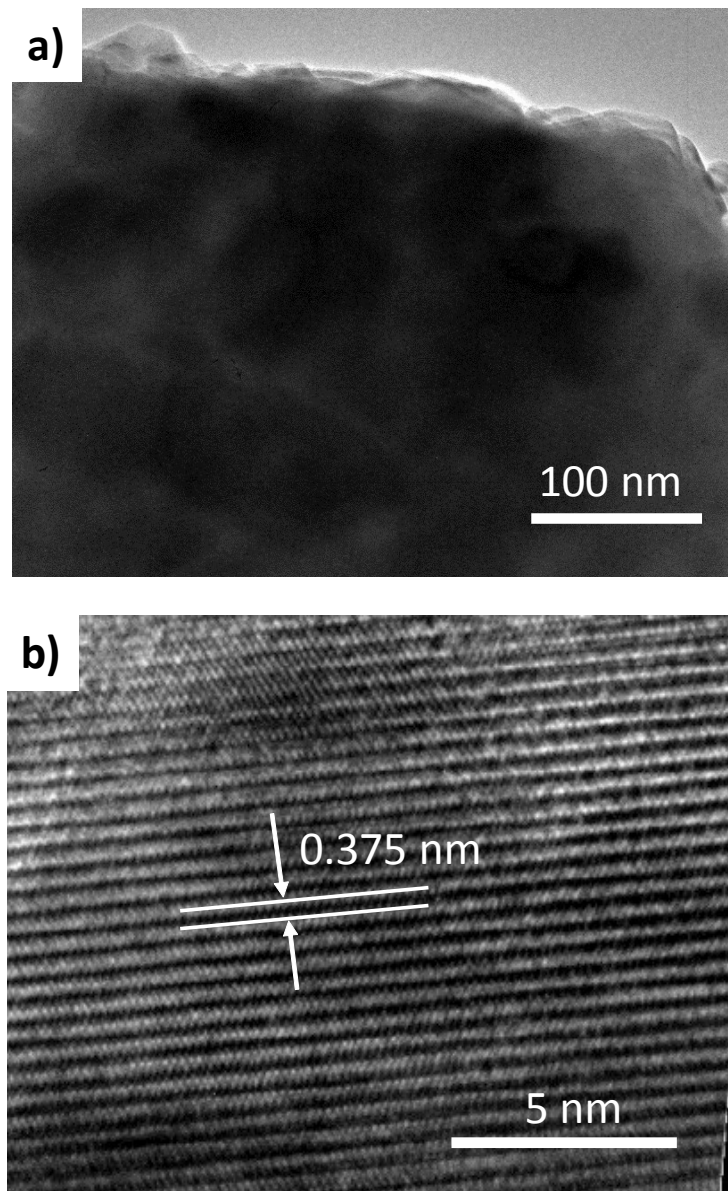


Fig. S3 TEM (a) and high-resolution TEM (b) images of CaMnO_3 .

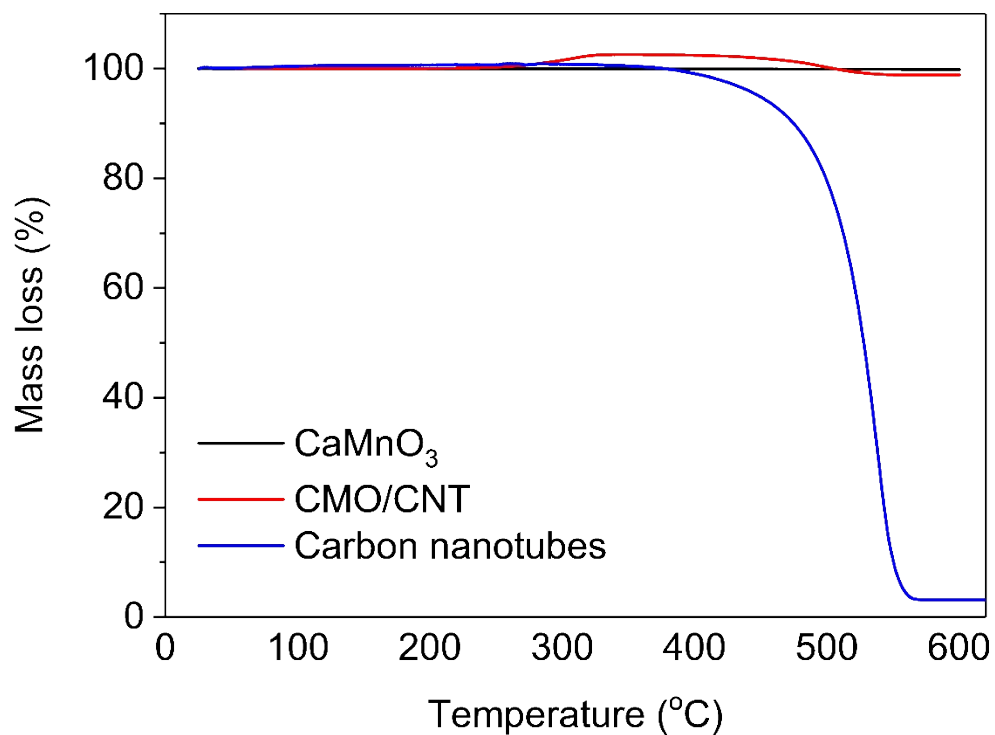


Fig. S4 TGA profile of CaMnO₃, CMO/CNT and carbon nanotubes in air. CMO/CNT (red) shows re-oxidation to stoichiometric CaMnO₃ (black), where no mass gain is observed in CaMnO₃. Pure carbon nanotubes (blue) burn off occurs above 350 °C and corresponds to the weight loss of carbon nanotubes in CMO/CNT.

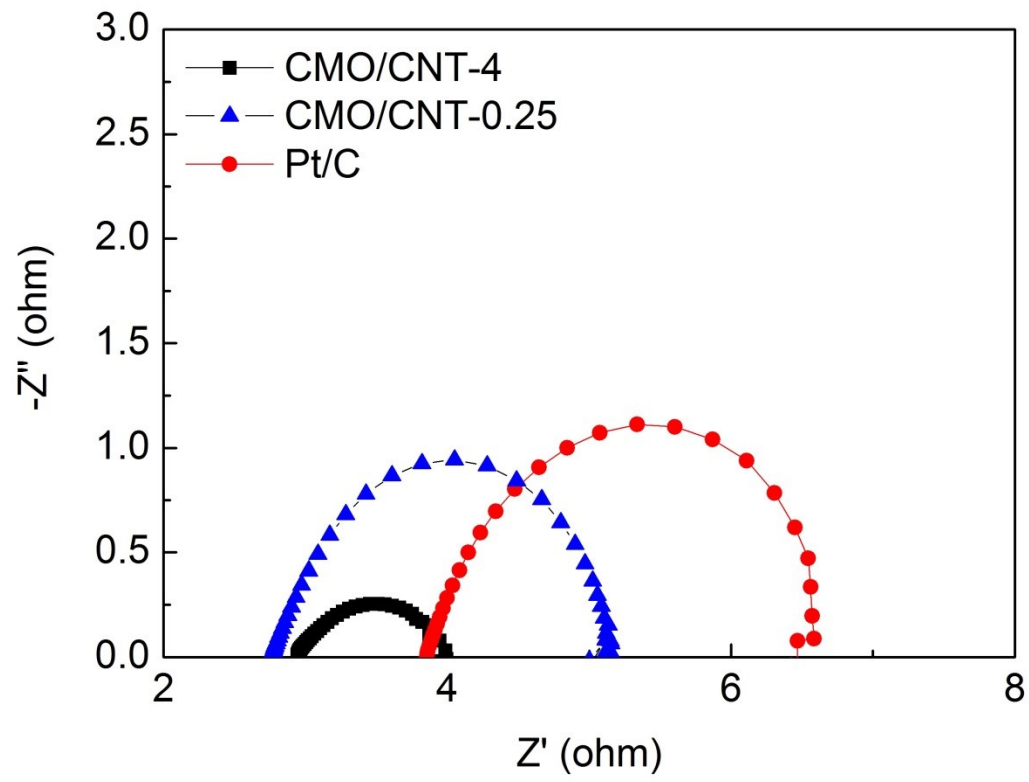


Fig. S5 Nyquist plot of zinc-air batteries with CMO/CNT-4, CMO/CNT-0.25 and Pt/C.

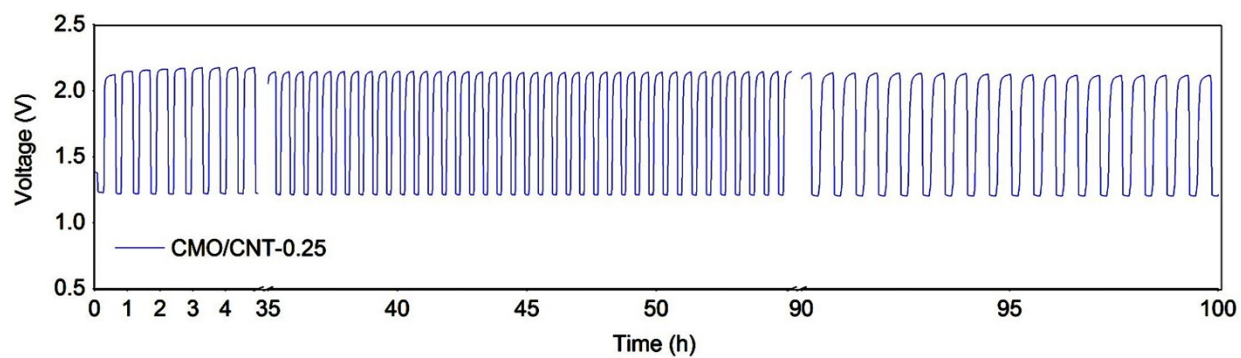


Fig. S6 Cycling stability performance of CMO/CNT-0.25 during galvanostatic recurrent pulse cycling test (discharging at 5 mA cm^{-2} for 10 min and charging at 2.5 mA cm^{-2} for 20 min in each cycle).

Table S1. Chemical states of Mn and O in $\text{CaMnO}_{3-\delta}$ and CMO/CNT.

	Mn $2p_{3/2}$			O 1s		
	Mn ³⁺	Mn ⁴⁺	Mn ³⁺ content	lattice oxygen	adsorbed oxygen	lattice oxygen content
	(eV)	(eV)	(%)	(eV)	(eV)	(%)
$\text{CaMnO}_{3-\delta}$	642.0	642.8	34.8	529.0	532.1	42.2
CMO/CNT	641.7	642.5	33.6	529.4	531.0	41.3

Table S2 Tabulated data for oxygen reduction reaction of the various electrocatalysts, with Pt/C as the benchmark

Catalyst	Oxygen reduction reaction activity	
	Onset potential at tangent (V, vs RHE)	Current density at 0.2 V (vs RHE) (mA cm ⁻²)
CaMnO ₃	0.76	-2.47
CMO/CNT	0.84	-4.27
Carbon nanotubes	0.72	-2.83
20 % Pt/C	0.89	-5.34